Final Report for AOARD Grant FA2386-11-1-4081

"**Composite Nanoshells for Enhanced Solar-to-Fuel Photocatalytic Conversion**"

Date 06/20/2012

Name of Principal Investigators: Tai-Chou Lee

- e-mail address : taichoulee@ncu.edu.tw
- Institution : Department of Chemical and Materials Engineering, National Central University
- Mailing Address : 300 Chung Ta Road, Chung-Li 320 Taiwan
- Phone : +886-3-4227151-34211
- Fax : +886-3-4252296

Period of Performance: 06/23/2011 – 06/23/2012

Abstract

In our preliminary study, we have prepared quaternary semiconductor powders of $Ag_xIn_xZn_yS_{2x+y}$ and varied the levels of indium content. The photocatalytic activity can be increased substantially. In this study, we further extended the investigation, fabricated the thin films of Ag-In-Zn-S compound semiconductor and measured the photoelectrochemical activities. By using electrophoretic deposition, the annealed powders of this quaternary solid solution were deposited on the ITO substrate. A larger photo-current density was measured by illuminating on the glass side when the film is thick. At 0 V v.s. SCE, the photo-current density is 0.137 mA/cm^2. SEM images show that the structure of the film is porous. The exposed area on ITO is expected to be the reactive sites when bias voltage is applied, with or without light irradiation. In a separate experiment, the metal oxide (SiO_2 or SnO_2) -coated nanoshells were synthesized. SnO_2-coated nanoshells provided enhanced stability at high pH. The effect of temperature and localized surface plasmon resonance, typically with addition of Ag@Au NPs (nanoparticles) was evaluated. Layered structure composed of nanoshell/SiO_2/ZnO was also studied. With/without silica layer, nanoshells (NSs) show totally different absorption peaks appeared in UV-vis spectrum. With the presence of nanoshells@SiO_2, the IR range in the solar spectrum can be fully utilized. The incorporation of nanoshell@SiO_2, as well as the nanostructure of photocatalyst will be further investigated.

Report Documentation Page

Form Approved
OMB No. 0704-0188

1. REPORT DATE	2. REPORT TYPE	3. DATES COVERED
27 JUN 2012	**Final**	**23-06-2011 to 22-06-2012**

4. TITLE AND SUBTITLE
Composite Nanoshells for Enhanced Solar-to-Fuel Photocatalytic Conversion

5a. CONTRACT NUMBER
FA23861114081

5b. GRANT NUMBER

5c. PROGRAM ELEMENT NUMBER

6. AUTHOR(S)
Tai-Chou Lee

5d. PROJECT NUMBER

5e. TASK NUMBER

5f. WORK UNIT NUMBER

7. PERFORMING ORGANIZATION NAME(S) AND ADDRESS(ES)
National Central University,No.300, Jhongda Rd,Jhongli City, Taoyuan 320,Taiwan,NA,NA

8. PERFORMING ORGANIZATION REPORT NUMBER
N/A

9. SPONSORING/MONITORING AGENCY NAME(S) AND ADDRESS(ES)
AOARD, UNIT 45002, APO, AP, 96338-5002

10. SPONSOR/MONITOR'S ACRONYM(S)
AOARD

11. SPONSOR/MONITOR'S REPORT NUMBER(S)
AOARD-114081

12. DISTRIBUTION/AVAILABILITY STATEMENT
Approved for public release; distribution unlimited

13. SUPPLEMENTARY NOTES

14. ABSTRACT
This is the report of a study to further investigate the fabrication of thin films of the compound semiconductor Ag-In-Zn-S. The researchers also measured the photoelectrochemical activities of these compounds.

15. SUBJECT TERMS
Metal Nanoshells, Metal Nanoshells, Photocatalysts, Hydrogen Generation

16. SECURITY CLASSIFICATION OF:			17. LIMITATION OF ABSTRACT	18. NUMBER OF PAGES	19a. NAME OF RESPONSIBLE PERSON
a. REPORT	b. ABSTRACT	c. THIS PAGE			
unclassified	**unclassified**	**unclassified**	**Same as Report (SAR)**	**10**	

Introduction

Of all known renewable energy sources, solar energy stands as the most abundant and readily accessible. Consider, for example, that the amount of solar energy striking the earth every 40 minutes is approximately equal to the amount of energy consumed globally on an annual basis.[1] From this perspective, the United States is fortunate to have vast tracts of land that are suitable for constructing solar power plants; in fact, in the desert Southwest alone there are an estimated 250,000 square miles of suitable land receiving more than 4,500 quadrillion British thermal units (Btu) of solar radiation per year.[1] Converting only 2.5% of that radiation into electricity would equal the total national energy consumption during all of 2006.[1]

The abundance and availability of solar energy has sparked the exploration of a wide variety of solar conversion technologies, including those based on photovoltaics (direct solar to electric), photothermal (solar to heat), and photosynthesis (solar to fuel). In the latter technology, artificial photosynthesis mimics natural photosynthesis by converting water and/or carbon dioxide into fuels and oxygen using sunlight. Splitting water to produce hydrogen and oxygen is one example, and it is the most promising replacement for fossil fuels without any pollutant[2-4]. The development of visible-light-driven photocatalysts for water splitting is critical. ZnS is a highly active photocatalyst for H_2 evolution under UV light irradiation[5-6]. Because of its wide band gap, the conduction band level is high enough to reduce water. $(AgIn)_xZn_yS_{2x+y}$ solid solution, derived from ZnS is a narrower band gap semiconductor. The absorption of the solid solutions can be tuned from UV light to visible light by adjusting $ZnS/AgInS_2$ ratio. $AgInZn_7S_9$ with a high efficiency of H_2 production is a typical example (~3.3 L/m^2-h).[7] $AgInZn_7S_9$ solid solution with 2.35 eV band gap absorbs the wavelength below 600 nm[8]. For wavelength longer than 600 nm, the light cannot be utilized effectively. This fact has motivated us to search for materials or composite materials that can utilize as much solar energy as possible.

Metal-metal nanoshells (Ag@Au) can absorb the light at different wavelength[9] by altering the thickness of nanoshell (Au). The nanoparticles have an absorption edge in the IR range (>700 nm) can convert the solar energy to heat. According to reaction kinetics, the water splitting reaction rate increases with the temperature. In this study, we wish to explore the development of a unique solar-to-fuel conversion system that is based on recent advances in nanotechnology. In the first part of the report, our second-generation photocatalysts were deposited onto ITO-coated glass substrates by electrophoresis. The photoelectrochemical activities of these films were measured. Secondly, we reported the novel synthesis of metal oxide (SiO_2 and SnO_2)-coated metal-metal nanoshells. These unique IR-absorption nanoparticles can be used as seeds to further deposit other metal oxide layer, e.g. ZnO in this study.

Experiment

1. *Preparation of photocatalyst*

An aqueous solution of $AgNO_3$ (J.T. Baker; 100 %), $In(NO_3)_3 \cdot xH_2O$ (Alfa Aesar; 99.99 %), $Zn(NO_3)_2 \cdot 6H_2O$ (J.T. Baker; 100 %) was prepared in a 100 mL round bottomed flask and mixed well. Thioacetamide (TAA, Merck; 99 %) was used as the S^{2-} source. Prescribed molar ratios in the precursor solution are listed in Table 1. After 5 h of reaction, the precipitates were collected by centrifugation, rinsed thoroughly with deionized (DI) water for several times, and then dried in an 80 °C oven for 12 h. The powders were heat treated at 800 °C for 1 h in an ultrapure N_2 atmosphere in a tube furnace. These powders were pulverized small enough to be suspended in isopropanol.

Table 1. Compositions of the precursor solutions.

Ag	In	Zn	TAA
1	1.75	7	10.5

2. *Electrophoretic deposition*

The powders (0.5 g) were then suspended in isopropanol (20 mL) and ultrasonicated for 10 min. Two pieces of ITO glasses (1 cm x 4 cm) were immersed in the suspension and applied a voltage (120 V) across these two electrodes. The distance between the two ITO was set at 1 cm, as shown in Figure 1. The depositing times were 5 s and 15 s. The deposited films were dried in the atmospheric condition and then baked at 450 °C for 1 h.

3. *Photoelectrochemical Reaction*

Photocatalytic reactions were conducted in a home-made glass cell with a quartz side window. The 300 W Xenon lamp was employed to simulate the sun light (Figure 2). The light was focused on the quartz side window with the intensity of 100 mW/cm^2. The photocatalyst film, as the working electrode, was placed in an aqueous solution containing sacrificial reagents (220 mL of 0.25 M K_2SO_3 and 0.35 M Na_2S) with magnetic stirring. They were then reacted under a Xe lamp and a bias voltage. The photo current, as well as the dark current were measured by using a potentiostat (CHI). The chopping method was employed to demonstrate the photocatalytic activities.

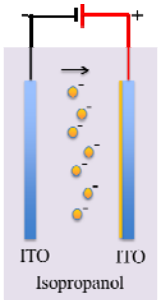

Figure 1. Electrophoretic deposition.

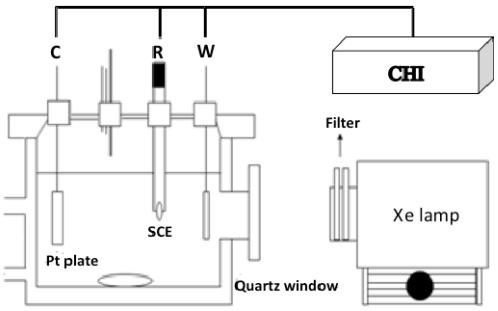

Figure 2. Photoelectrochemical reaction system.

4. *Preparation of Silver nanoparticles (NPs)*

Silver NPs were prepared by using the slightly modified Lee and Meisel method[10]. A solution of 1 mM $AgNO_3$ (100 mL) in a 250 mL flask was heated, and 2 mL of 1 % sodium citrate (Sigma Aldrich) solution was added as soon as the $AgNO_3$ solution began boiling[9]. The yellowish solution turned to greenish after the addition trisodium citrate. After 45 min of reaction, the Ag NPs were collected by centrifuge for 20 min at 4000 rpm (3 times). Ag NPs were then re-suspended and filtered them through 0.22 μm membrane filter to remove the Ag nanorods. The SEM image (Figure 3) shows that the size of Ag NP is 60 ~ 80 nm.

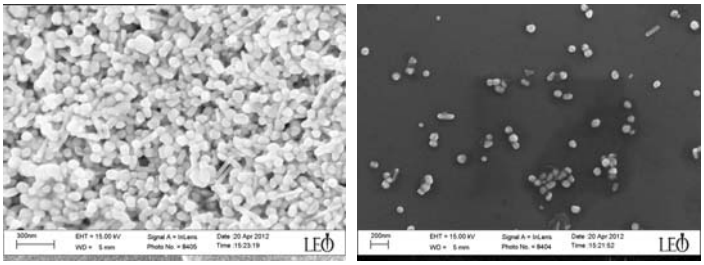

Figure 3. SEM images of Ag NPs. The size is around 60~80 nm.

5. *Gold nanoshell growth*

K-Gold solution was prepared by dissolving 0.025 g of K_2CO_3 (J.T. Baker; 99.8 %) in a mixture of water (100 mL)[11-12]. After stirring for 10 min, an aliquot (1 %, 2 mL) of $HAuCl_4$ solution was added. The solution changed from yellow to colorless in 30 min, and then kept in dark refrigerator for 24 h. An aliquot (8 mL) of K-Gold solution was placed in a 20 mL qorpak containing a magnetic stirring bar, and then varying amounts of silver NPs were added to produce gold shells of various thicknesses. After washing with DI water for several times, NSs were re-suspended for further experiments.

6. *Silica layer coating*

Silica layer was coated on top of the nanoshells by using sol-gel process with a mixture containing nanoshells (5 mL), water (5 mL), ethanol (22 mL), ammonia (2 mL) and Tetraethyl orthosilicate (TEOS, 25 μL). The solution was kept overnight with stirring. Various amounts of TEOS were added into the solution to generate different silica thicknesses. The particles were then washed with DI water by centrifugation for few times, and were then re-suspended in DI water. Figure 4 shows two thicknesses prepared from this procedure.

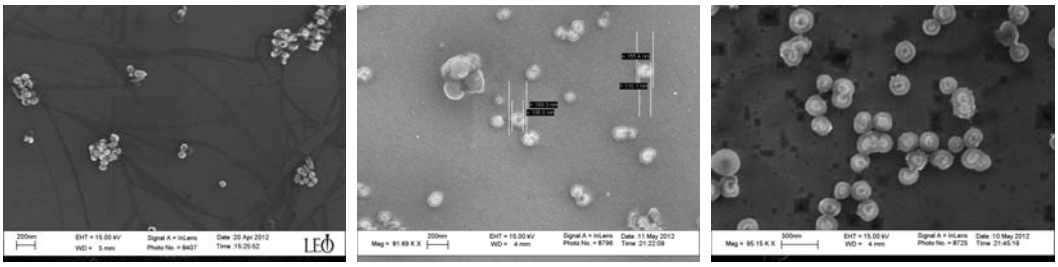

Figure 4. Gold NSs (left); Gold NS@silica, 20 nm (middle), 50 nm (right)

7. *ZnO layer coating*

0.0075 g of zinc nitrate hexahydrate (J.T. Baker; 100 %) was dissolved into 10 mL of distilled water and generated a white precipitate of zinc hydroxide [$Zn(OH)_2$] after adding 1 mL (1M) of sodium hydroxide solution. This solution was added to 1 mL NSs suspension under stirring for 3-4 min. Finally, this solution was kept at 90-95 °C for 30 min under stirring. NS@SiO_2@ZnO or NS@ZnO multilayer nanocomposites were synthesized (see Figure 5)

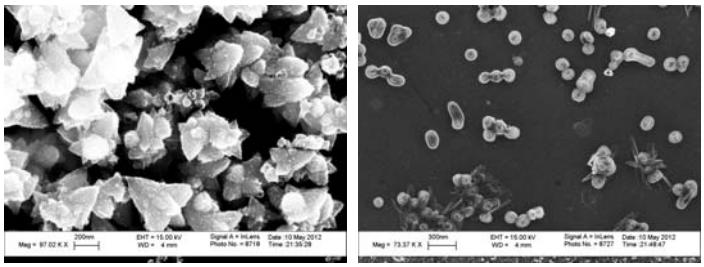

Figure 5. ZnO coated, on nanoshell (left); on nanoshell@silica (right)

Results and Discussion

In published papers,[7, 13] the amount of zinc sulfide was considered the major parameter to adjust the band gap energy of $Ag_xIn_xZn_yS_{2x+y}$. The position of conduction band relates to the efficiency of hydrogen production and is determined by the band gap energy. In our preliminary study, we have increased the activity of Ag-In-Zn-S by changing the levels of indium contents. By adjusting indium and zinc, we were able to optimize the compositions of this quaternary photocatalyst for a better solar-to-fuel efficiency. In the first section, we chose the powders with highest photocatalytic activity to deposit onto ITO glass. Before electrophoretic deposition, the physical properties of the photocatalysts were first characterized. Figure 6 (left) shows hydrogen evolution rate of 340 μmol/h with Pt co-catalyst. The XRD spectrum (Figure 6 (middle)) shows this sample with a typical hexagonal structure of Ag-In-Zn-S. Finally, Figure 6 (right) demonstrates that this material is indeed visible light active. The absorption edge locates at approximately 500 nm, corresponding to band gap energy of 2.4 eV

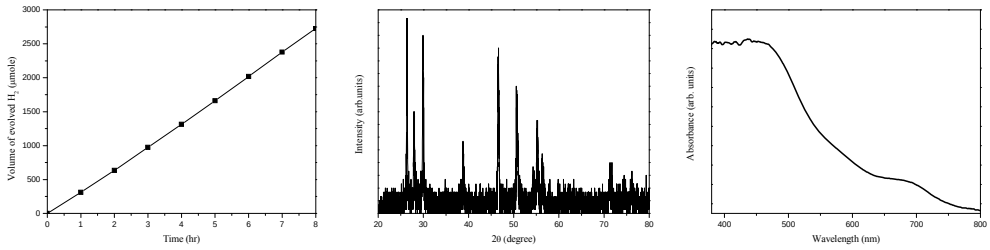

Figure 6. Physica properties of the powders used for electrophoretic deposition. The hydrogen evolution of Pt-cocatalyst (left); XRD spectrum (middle); UV-VIS spectrum (right)

Figure 7 shows the photoelectrochemical activities of the film prepared from electrophoretic deposition for 15 s. The linear sweep voltammogram, from -1 V to 0.4 V v.s. SCE, was recorded using chopping method (Figure 7a). The photocurrent density of this material is the difference between light and dark condition. Note that dark current rose dramatically at 0.2 V, perhaps due to the severe recombination of generated electron-hole pairs at the electrolyte-semiconductor interface. In order to further understand the charge transport behavior, we first simply irradiate the light on the ITO glass side and on the photocatalyst side with the bias voltage set at 0 V v.s. SCE. On the glass side, the photocurrent density is about 0.137 mA/cm^2, almost 6 times higher than 0.024 mA/cm^2 irradiated on the photocatalyst side. These data strongly suggested that this porous thin film suffers a huge loss due to the leakage current through ITO glass substrate under bias.

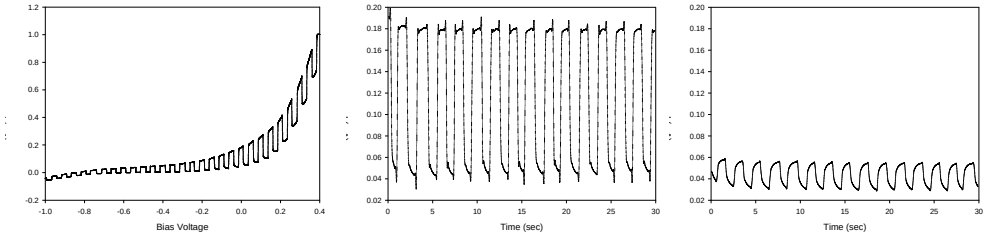

Figure 7. Photocurrent density (a) at applied voltages from -0.1 V to 0.4 V; (b) irradiated on glass side at 0 V; (c) irradiated on photocatalyst side at 0 V

The thickness is another key factor causing different photoelectrochemical activities between the glass side and catalyst side. SEM images show the morphology on a large scale. It seems that the films are rather uniform (Figure 8 (left)). However, there are still some porous structures observed at local areas. The thickness of film is around 22 μm (Figure 8 (right)) and composed of the particles ranging from 100 nm to 1 μm with irregular shapes (Fig. 8 (middle)). Illuminating on photocatalyst side, the film is too thick for the light to penetrate the whole film. Take the typical absorption coefficient of 10^{-5} /nm of this material, the thickness required to absorb 99% of the light is in the range of 1 μm. Electron-hole pairs generated might have been trapped or recombined before reaching the ITO-semiconductor interface. The long distance that the electrons must diffuse through increases the probability of recombination. On the contrary, when the light irradiates on the glass side, electrons can be removed easily under bias, and the holes can react with sacrificial reagent. As a whole, our Ag-In-Zn-S solid solution films also have specific nanostep structures.[7] The edges on the photocatalysts surface are considered as active sites for photocatalytic reactions.[7]

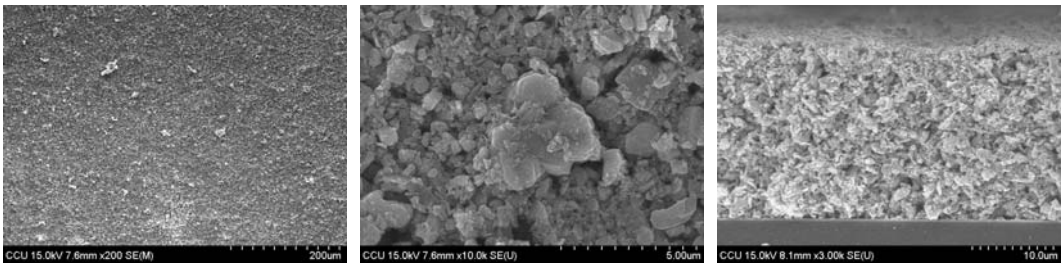

Figure 8. SEM images of the film with low resolution (left), high resolution (middle), and cross section (right)

As part of our efforts to incorporate light-absorbing nanoparticles into thin-film solar-to-hydrogen fuel cells, we have been exploring the synthesis and stability of SnO_2-coated gold nanoparticles and nanoshells. Figure 9 shows a TEM image of some sample particles, where the shell/core morphology can be readily discerned. In addition, Figure 10 illustrates the enhanced stability of these particles at high pH when compared to analogous (and much better known) SiO2-coated gold nanoparticles.

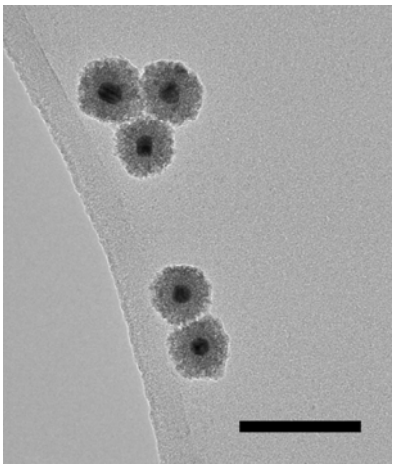

Figure 9. TEM image of SnO_2-coated Au Au nanoparticles (100-nm scale bar).

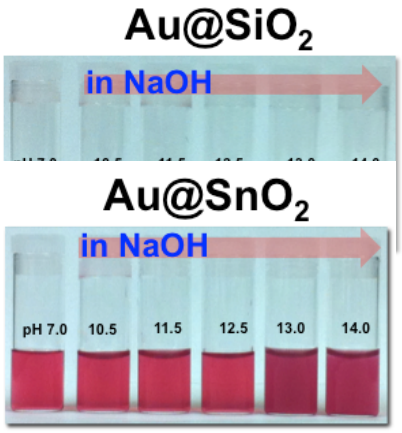

Figure 10. Colloidal stability as a function of solution pH.

In more recent work, we have synthesized gold nanoshells (GNS) at dimensions ranging from 100–200 nm and are exploring their ability to effect photothermal heating of the ambient environment in an effort to enhance the catalytic activity of the system. Figure 11 shows an SEM image of ~125 nm gold nanoshells. We also evaluated the photothermal properties of the nanoshells described in our previous report (~200 nm diameter). When the latter nanoshells were irradiated in aqueous solution with a laser at 808 nm, the temperature of the solution increased from 24 °C to 38 °C over 10 min (Figure 12), demonstrating effective photothermal heating.

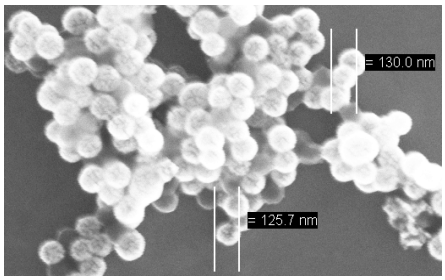

Figure 11. SEM image of ~125 nm Au nanoshells.

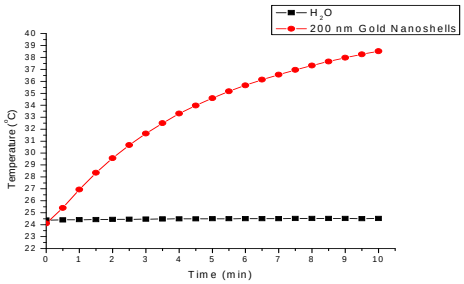

Figure 12. Heating with 200 nm Au nanoshells.

In a separate experiment, the gold nanoshells (NSs) were further coat with ZnO. In order to prevent the excited electrons from transferring to the NSs, the silica was coated on top of NSs. The absorption spectra (Figure 13) show little difference between SiO_2-coated nanoshells and bare nanoshells. However, the absorption spectra are totally different with and without SiO_2 layer after ZnO coating (see Figure 14). The color of the solution containing NSs without SiO_2 changes from dark blue

to black, whereas the color the solution containing of NSs with SiO_2 remains the same. We will continue to incorporate metal NSs into our photocatalytic system. Our strategies are, 1: synthesize uniform distributed NSs@SiO_2, and 2. Create a NSs core/photocatalysts shell structure. Solar energy in the visible-light range is expected to be absorbed by the photocatalyst first without any interference of the metal nanoshells. These topics are under investigations.

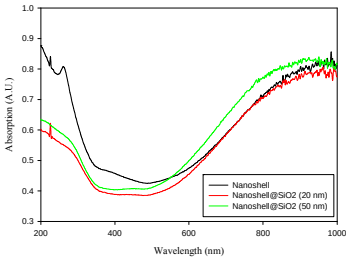

Figure 13. Absorption of SiO2-coated nanoshells.

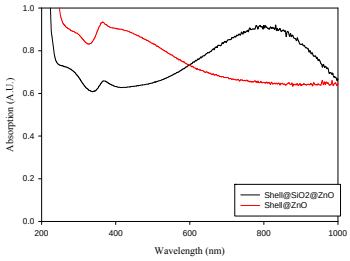

Figure 14. Absorption of core-shell particle (nanoshell@SiO_2@ZnO)

In summary, we have prepared Ag-In-Zn-S photocatalytic particle films by electrophoretic deposition. The highest photocurrent density of 0.137 mA/cm^2 at 0 V (v.s. SCE) was obtained under 100 mW/cm^2 illumination. We can further tune the [Zn]/[Ag] ratio to determine the maximum utilization of solar energy, in order to achieve higher solar-to-fuel conversion efficiency. Secondly, we have reported the synthesis of metal oxide (SiO_2 and SnO_2)-coated nanoshells. These metal oxide-coated nanoshells, especially SnO_2-coated ones exhibit superior stability over a wide range of pH. In the future study, we will integrate these two import findings and create various core-shell structures. The next phase of the research is to utilize localized surface plasmon resonance generated by nanoshells, incorporate into our photocatalytic system, and study the solar-to-fuel conversion efficiency.

Reference

1. Zweibel, K.; Mason, J.; Fthenakis, V., *Sci. Am.* **2008**, Jan., 64-73.
2. Kudo, A., *Int J Hydrogen Energ* **2007,** *32*, 2673-2678.
3. Kudo, A.; Sekizawa, M., *Chemical Communications* **2000**, 1371-1372.
4. Chen, D.; Ye, J., *Journal of Physics and Chemistry of Solids* **2007,** *68*, 2317-2320.
5. Reber, J.-F.; Meier, K., *Journal of Physical Chemistry* **1984,** *88*, 5903-5913.
6. Zeug, N.; Bucheler, J.; Kisch, H., *J Am Chem Soc* **1985,** *107*, 1459-1465.
7. Tsuji, I.; Kato, H.; Kobayashi, H.; Kudo, A., *J. Am. Chem. Soc.* **2004,** *126*, 13406-13413.
8. Tsuji, I.; Kato, H.; Kobayashi, H.; Kudo, A., *J Am Chem Soc* **2004,** *126*, 13406-13413.
9. Yang, Y.; Shi, J. L.; Kawamura, G.; Nogami, M., *Scripta Mater* **2008,** *58*, 862-865.
10. Lee, P. C.; Meisel, D., *The Journal of Physical Chemistty* **1982,** *86*, 3391-3395.

11. Ji, X. J.; Shao, R. P.; Elliott, A. M.; Stafford, R. J.; Esparza-Coss, E.; Bankson, J. A.; Liang, G.; Luo, Z. P.; Park, K.; Markert, J. T.; Li, C., *J Phys Chem C* **2007,** *111*, 6245-6251.

12. Phonthammachai, N.; Kah, J. C. Y.; Jun, G.; Sheppard, C. J. R.; Olivo, M. C.; Mhaisalkar, S. G.; White, T. J., *Langmuir* **2008,** *24*, 5109-5112.

13. Kudo, A.; Tsuji, v.; Kato, H., *Chem. Commun.* **2002**, 1958-1959.